Received: 17 January 2020 | Accepted: 28 August 2020

DOI: 10.1111/1365-2435.13672

RESEARCH ARTICLE

Functional Ecology | BRITISH ECOLOGICAL SOCIETY

Vector demography, dispersal and the spread of disease: Experimental epidemics under elevated resource supply

Alexander T. Strauss | Jeremiah A. Henning | Anita Porath-Krause | Ashley L. Asmus | Allison K. Shaw | Elizabeth T. Borer | Eric W. Seabloom

Department of Ecology, Evolution, and Behavior, University of Minnesota, St. Paul, MN, USA

Correspondence
Alexander T. Strauss
Email: straussa@umn.edu

Present address
Alexander T. Strauss, Odum School of Ecology, University of Georgia, Athens, GA, USA
Jeremiah A. Henning, Department of Biology, University of South Alabama, Mobile, AL, USA

Funding information
Division of Environmental Biology, Grant/Award Number: 1556649; Division of Integrative Organismal Systems, Grant/Award Number: 1556674

Handling Editor: Arjen Biere

Abstract

1. The spread of many diseases depends on the demography and dispersal of arthropod vectors. Classic epidemiological theory typically ignores vector dynamics and instead makes the simplifying assumption of frequency-dependent transmission. Yet, vector ecology may be critical for understanding the spread of disease over space and time and how disease dynamics respond to environmental change.
2. Here, we ask how environmental change shapes vector demography and dispersal, and how these traits of vectors govern the spatiotemporal spread of disease.
3. We developed disease models parameterised by traits of vectors and fit them to experimental epidemics. The experiment featured a viral pathogen (CYDV-RPV) vectored by aphids *Rhopalosiphum padi* among populations of grass hosts *Avena sativa* under two rates of environmental resource supply (i.e. fertilisation of the host). We compared a *non-spatial* model that ignores vector movement, a *lagged dispersal* model that emphasises the delay between vector reproduction and dispersal, and a *travelling wave* model that generates waves of infections across space and time.
4. Resource supply altered both vector demography and dispersal. The *lagged dispersal* model fit best, indicating that vectors first reproduced locally and then dispersed globally among hosts in the experiment. Elevated resources decreased vector population growth rates, nearly doubled their carrying capacity per host, increased dispersal rates when vectors carried the virus, and homogenised disease risk across space.
5. Together, the models and experiment show how environmental eutrophication can shape spatial disease dynamics—for example, homogenising disease risk across space—by altering the demography and behaviour of vectors.

KEYWORDS
barley/cereal yellow dwarf virus, behaviour, disease ecology, dispersal, eutrophication, spatial, transmission, vector

1 | INTRODUCTION

The spread of vector-borne disease depends on the demography, dispersal and behaviour of vectors. However, vector dynamics are often omitted from disease models for simplicity. For example, classic models assume that vector transmission is proportional to the frequency of infections in host populations (Antonovics et al., 1995; Chan & Jeger, 1994; Keeling et al., 2007). Yet, arthropod vectors are foraging animals, and new predictions can arise from models that incorporate their demography (Shaw et al., 2017;

Sota & Mogi, 1989), preferences among hosts (Kingsolver, 1987; Shoemaker et al., 2019), feeding behaviour (Madden et al., 2000), dispersal (Chamchod & Britton, 2011; Chao et al., 2013; Donnelly et al., 2019; Shaw et al., 2019) and interactions with natural enemies (Crowder et al., 2019). Thus, treating vectors as interacting members of ecological communities rather than invisible agents of disease enriches general insights and may improve predictions for future outbreaks of disease.

Vector ecology may be especially critical for understanding spatial disease dynamics and consequences of environmental change. The spread of any species over space and time depends on its reproduction and dispersal (Bjørnstad et al., 2002; Hastings et al., 2005; Skellam, 1951). For vectors, these processes also can govern the spread of infections. For example, diseases can spread faster when mosquitos (Russell et al., 2005), ticks (Walter et al., 2016), aphids (Irwin & Thresh, 1988) and other arthropod vectors (Evans, 2016) disperse farther. Consequently, variation in vector and/or host movement can create a variety of spatiotemporal patterns, ranging from homogeneous disease incidence across space (Foley et al., 2016) to travelling waves of infection (Comeau & Dubuc, 1977; Cummings et al., 2004; Menkis et al., 2016). In addition to explaining these spatial patterns, vector ecology is also a critical conduit through which environmental change can shape disease. For example, the demography of vectors can respond to climate change (Githeko et al., 2000), land use change (Pope et al., 2005) and environmental eutrophication (Comeau & Dubuc, 1977; Schrama et al., 2018; Zehnder & Hunter, 2009). In a world undergoing rapid, multifaceted environmental change, incorporating such effects into disease forecasts is becoming increasingly important.

Despite the potential for environmental change to alter spatiotemporal disease dynamics via vector demography and dispersal, few experiments track interactions among hosts, vectors and pathogens across space and time under differing environmental conditions. In animal systems, hosts and vectors (e.g. ticks or mosquitoes) are both mobile, and, for many hosts, creating and tracking experimental epidemics may be unethical or infeasible. For example, recapture rates for mosquitos are generally low (Marini et al., 2010; Russell et al., 2005), kissing bugs that vector Chagas disease are difficult to sample (Abad-Franch et al., 2010) and contacts between ticks and hosts must often be inferred from infection data (Foley et al., 2016; Walter et al., 2016). In contrast, plant hosts are stationary, making them much easier to track. Moreover, many diseases in wild plants, agricultural crops and forests are transmitted by insect vectors (Comeau & Dubuc, 1977; Evans, 2016; Seabloom et al., 2013), and relevant environmental change (e.g. nitrogen deposition and eutrophication) can be easily manipulated for plant hosts via fertilisation. Thus, many plant–pathogen systems are well-suited to develop and test models that incorporate vector ecology into spatiotemporal theory for disease (Jeger et al., 2018).

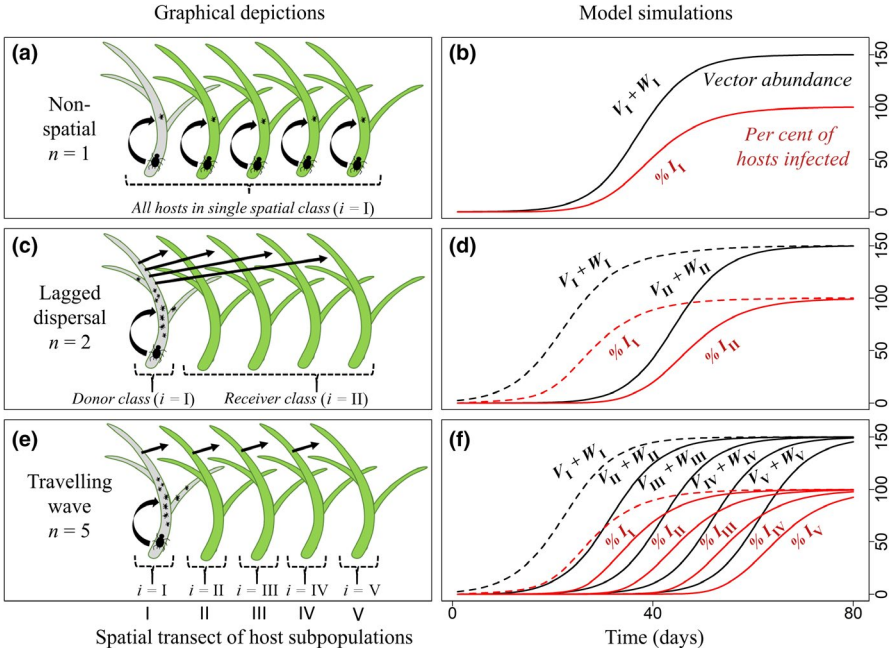

FIGURE 1 Three models for the spread of vectors and disease among sessile hosts. Graphical depictions (left) illustrate the spread of vectors along a transect of five hosts (I–V) under three spatiotemporal scenarios: *non-spatial* vector dynamics (top), *lagged dispersal* (middle) and a *travelling wave* (bottom). Model simulations (right) track the abundance of vectors per host (sum of infectious [*W*] and non-infectious [*V*] vectors; black) and percent of hosts infected (%*I*; red) in each spatial class (*i*). ***Non-spatial***: (a) Vectors reproduce synchronously and (b) all hosts belong to one spatial class ($n = 1$) with increasing vectors and infections over time. ***Lagged dispersal***: (c) Vectors disperse from an initial 'donor' host (grey) to all 'receiver' hosts (green). (d) Hosts are split into two spatial classes ($n = 2$), with vectors and infections of the receivers (solid lines; $i = 2$) lagging behind the donors (dashed; $i = 1$). ***Travelling wave*:** (e) Vectors disperse along the transect of hosts in a wave. (f) Hosts are divided into five spatial classes ($n = 5$), with vectors and infections of each class (*i*) lagging behind the previous class ($i - 1$). Parameters: $K = 150$ vectors host^{-1}, $r = 0.2$ day^{-1}, $d = 0.01$ day^{-1}, $\beta_{VH} = 0.001$ hosts vector^{-1} day^{-1}, $\beta_{VH} = 0.68$ arenas host^{-1} day^{-1}

Here we develop mathematical models grounded in vector demography and dispersal and fit them to experimental epidemics of a viral pathogen (B/CYDV) vectored by aphids *Rhopalosiphum padi* among grass hosts *Avena sativa*. In the experiment, we track the spread of vectors and infections across populations of 100 hosts for 8 weeks (~4 to 5 aphid generations) under two rates of environmental resource supply (i.e. fertilisation of the host). Then we fit models to the data to ask whether elevated resource supply altered vector demography, dispersal or disease dynamics. We contrasted the fit of three models (Figure 1). First, a null *non-spatial* model ignored vector movement. Second, a *lagged dispersal* model emphasised the lag between vector reproduction and dispersal. Third, a *travelling wave* model generated waves of infection across space. We found that the *lagged dispersal* model fit best, indicating that vectors first reproduced on 'donor' hosts and then dispersed to all other 'receiver' hosts in the experiment. Elevated resource supply slowed vector population growth rates, nearly doubled the carrying capacity of vectors per host, accelerated dispersal rates when vectors carried the virus and homogenised disease risk over space. This combination of model and experiment highlights the importance of vector demography and dispersal for spatiotemporal disease dynamics and delineates impacts of relevant environmental change on this plant–aphid–virus system.

2 | MATERIALS AND METHODS

2.1 | Study system

Barley and cereal yellow dwarf viruses (B/CYDVs) infect over 150 species of grasses and cause substantial losses to cereal crops worldwide (Comeau & Dubuc, 1977; Irwin & Thresh, 1990). B/CYDVs are obligately transmitted among grasses by aphid vectors. The cosmopolitan aphid, *R. padi*, efficiently transmits several B/CYDV species including CYDV-RPV (hereafter: RPV). Epidemics in temperate regions begin when infectious (viruliferous) winged aphids (alates) aerially disperse from warmer climates and infect susceptible hosts (Irwin & Thresh, 1988). The virus then spreads locally from this focal point of infection as unwinged (apterous) aphids are born, acquire the virus by feeding on infected phloem and disperse to nearby plants (Bailey et al., 1995; Comeau & Dubuc, 1977; Irwin & Thresh, 1990). This process of local disease spread therefore depends on both aphid demography and dispersal (Skellam, 1951). Aphid fecundity is often higher on infected plants (Bosque-Perez & Eigenbrode, 2011), but this effect can reverse depending on host genotype (Jimenez-Martinez et al., 2004).

Enhanced resource supply could shape the local spread of B/CYDVs in several ways (Figure 2). Phosphorus fertilisation increases infection prevalence of several B/CYDV species in the field (Seabloom et al., 2013). However, phosphorus *reduces* infection prevalence of RPV when plants are exposed to a fixed number of aphids in the laboratory (Lacroix et al., 2014), perhaps by fuelling host defences against viruses. Thus, fertilisation can decrease per-aphid transmission. Nitrogen fertilisation typically enriches plant tissue chemistry and can increase aphid fecundity (Borer et al., 2009) and the number of aphids per plant (Comeau & Dubuc, 1977; Hamback et al., 2007). However, nitrogen can also inhibit aphid reproduction (Bogaert et al., 2017), especially in combination with phosphorus (Zehnder & Hunter, 2009), likely by boosting defences of plants against aphids. Thus, fertilisation might shape disease spread by altering the population growth rate and/or carrying capacity of vectors. If fertilisation alters aphid demography, it could also change the number of aphids dispersing to susceptible plants, assuming either constant (Lombaert et al., 2006) or increasing per-capita dispersal with higher aphid density (Tokunaga & Suzuki, 2008). These multiple potential impacts of elevated resources on disease have not been clearly delineated during epidemics (see Figure 2).

2.2 | Experiment

We tracked the spatiotemporal spread of aphid vectors (*R. padi*) and viral infections (RPV) through populations of grass hosts (cultivated oats: *A. sativa*) and asked whether fertilisation or presence of the virus altered vector demography and/or dispersal. Each experimental 'arena' (20 arenas total) contained 100 hosts arranged in a 10-by-10 grid (30 × 30 cm) of pots (60 mm tall, 27 mm diameter, 55 ml per pot). In each pot, we planted one seed (cv Coast Black oat, National plant germplasm system, USDA) in sterilised, nutrient-free, water-saturated media (70% medium vermiculite [Sun Gro Horticulture], 30% Turface MVP [Turface Athletic] by volume). We planted extra pots to replace hosts that would be sampled destructively during the experiment. This influx of a few susceptible hosts (4% per week) is unlikely to have influenced disease spread, as models indicated that the aphids dispersed globally throughout the arenas (see Section 3). Each arena was isolated in a mesh 'bug dorm' (32.5 × 32.5 × 77 cm; 160 μm mesh; MegaView Science Co.), grown in a climate-controlled room (23°C; 16:8 light:dark; 2× 40 W cool white fluorescent bulbs), and watered twice per week (500 ml distributed evenly among the 100 plants). Two weeks after planting the seeds, when most plants had grown two leaves, we began the experiment.

The experiment crossed two levels of resource supply (unfertilised [−R] or fertilised [+R]) with two levels of disease (with [+D] or without [−D] the virus). We replicated each combination of treatments five times, for a total of 20 arenas. We watered plants with modified Hoagland's nutrient solutions that differed only in their levels of nitrogen and phosphorus (0.1 or 5% dilutions; 50× differences; see Appendix). All aphids originated from the same continuously maintained culture. The virus was originally isolated in New York state (Appendix). For each arena, we placed 10 aphids in a vial, starved them for 2 hr and then added a 5 cm piece of oat tissue, either healthy or infected with RPV. Once the aphids began feeding

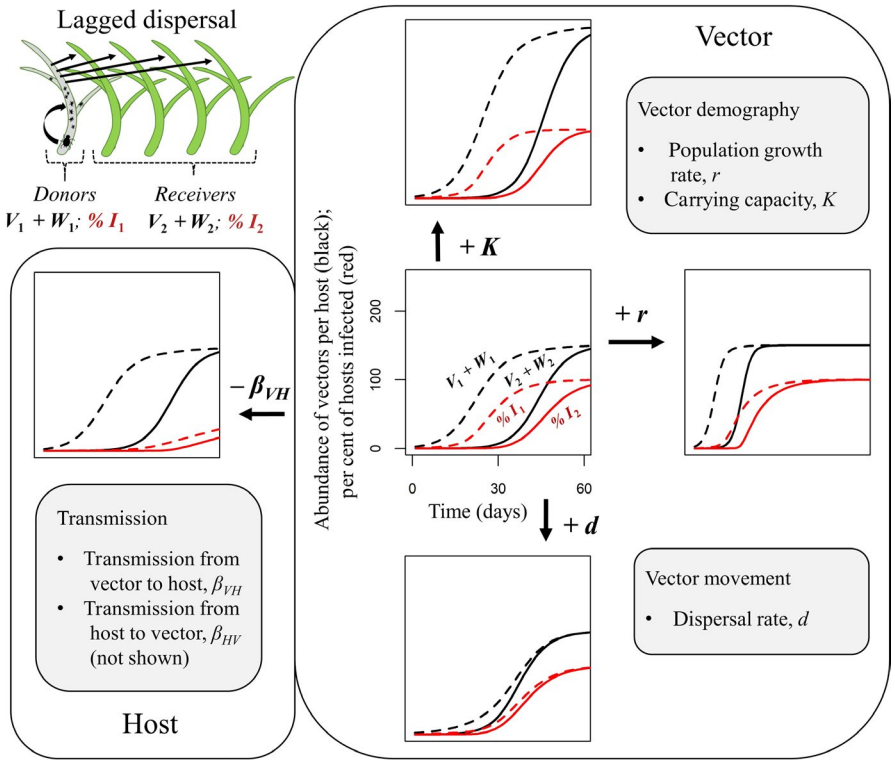

FIGURE 2 Four ways that elevated resource supply could shape disease dynamics via vector ecology. Simulations track total vector abundance and infection prevalence in donor hosts ($V_1 + W_1$ and $\%I_1$ [dashed]), and receiver hosts ($V_2 + W_2$ [solid black]; $\%I_2$ [solid red]) with *lagged dispersal*. Compared to a baseline (centre), elevated resource supply could alter disease dynamics by changing vector demography, dispersal and/or transmission (see 'Study system' in Section 2). Higher **carrying capacity** (K; top) could raise the abundance of vectors per host. Faster **population growth rate** (r; right) could accelerate the accumulation of vectors and infections. Faster vector **dispersal rate** (d; bottom) could homogenise disease dynamics across space. Reduced **transmission coefficients** from vector to host (β_{VH}; left) could slow disease spread independently of vector ecology. Parameters (contrasts in parentheses): $K = 150$ vectors host^{-1} (top = 250), $r = 0.2$ day^{-1} (right = 0.6), $d = 0.01$ day^{-1} (bottom = 0.1), $\beta_{VH} = 0.001$ hosts vector^{-1} day^{-1} (left: 0.0001), $\beta_{VH} = 0.68$ arenas host^{-1} day^{-1}

on the healthy tissues (~3 hr), we transferred them to the centre of their arenas. We allowed aphids to feed on the infected tissues for a standard 48-hr period to acquire the virus before transferring them. This slight difference in timing is unlikely to have biased our results (Appendix; Figure S1).

We sampled four plants from each arena weekly for 8 weeks (4–5 generations of aphids; spatial design shown in Figure S2). We never sampled the four plants in the centres of the arenas (Roman numeral I; where we added the aphids) because we could not re-sample this spatial class for 8 weeks (only four plants), and their removal could have exerted large effects on the initial aphid populations. Instead, we randomly sampled one host from each of four concentric 'rings' radiating outward from the centre (I), including plants in rings II (eight plants total), III (20 plants), IV (28 plants) and V (36 plants; perimeter of the arena). Each week, we counted the number of aphids on each plant with a dissecting microscope and determined whether the plant was infected by flash-freezing its tissue, extracting RNA, synthesising cDNA and testing for the presence of the virus via PCR (see Appendix for details). We replaced all sampled plants with healthy hosts of the same age, and only sampled plants that had been present for the entire duration of the experiment.

2.3 | Models

We developed spatiotemporal disease models grounded in vector demography and dispersal. Such models could help predict disease dynamics across broader spatial scales and under scenarios of global change by explicitly linking disease to vector ecology (Jeger et al., 2018). Therefore, instead of analysing our experiment with traditional statistical models, we developed general dynamical models and fit them to our data.

We developed three ordinary differential equation models that track changes in the densities of susceptible hosts (S), infected hosts (I) and vectors per host (V). The models differ in the number of spatial classes of hosts (n) and could become more or less appropriate at different scales (Figure 1). First, the simplest *'non-spatial'* model assumes that vectors distribute among all hosts and reproduce synchronously across the host population. This model only includes one homogeneous spatial class of hosts ($n = 1$; Figure 1a,b). Second, the *'lagged dispersal'* model assumes that vectors reproduce first on 'donor' hosts (centre of the experimental arenas) and then disperse globally to all other 'receiving' hosts (all sampled hosts in the experiment). This hypothesis of global dispersal seems reasonable given the spatial scale of the experiment (Bailey et al., 1995). This model

includes an additional dispersal parameter and two spatial classes of hosts: donors and receivers ($n = 2$; Figure 1c,d). Third, the *'travelling wave'* model assumes a series of lags as vectors reproduce and disperse between neighbouring hosts. Since our experiment includes five distinct spatial classes (centre of the arenas [I] and concentric rings radiating outward [II–V]), we fit the travelling wave model to five classes of hosts ($n = 5$; Figure 1e,f).

All three spatiotemporal scenarios are described by the general template of equations,

$$\frac{dV_i}{dt} = r(V_i + W_i)\left(1 - \frac{V_i + W_i}{K}\right) - dV_i + dV_{m,i} - \beta_{HV} V_i I_i, \quad (1)$$

$$\frac{dW_i}{dt} = \beta_{HV} V_i I_i - dW_i + dW_{m,i}, \quad (2)$$

$$\frac{dS_i}{dt} = -\beta_{VH} S_i W_i, \quad (3)$$

$$\frac{dI_i}{dt} = \beta_{VH} S_i W_i, \quad (4)$$

for $i = 1, \ldots, n$, with non-infectious vectors (V), infectious vectors (W), susceptible hosts (S) and infected hosts (I) indexed by their spatial class (i; parameters defined in Table 1). Vectors grow logistically with a population growth rate (r) and per-host carrying capacity (K). In this study system, all vectors are born uninfectious, and hosts cannot recover from infection (Irwin & Thresh, 1990). Separate transmission coefficients regulate transmission from host to vector (β_{HV}) and from vector to host (β_{VH}). Rather than assuming frequency-dependent transmission (Keeling et al., 2007), we allow transmission to depend on the abundance of infectious vectors per host. We assume that all vectors emigrate from hosts with a constant per-capita dispersal rate, d (Lombaert et al., 2006).

TABLE 1 Definitions and units for state variables and parameters of the models

Symbol	Definition	Units
V	Abundance of non-infectious vectors	Vectors host^{-1}
V_m	Abundance of immigrating non-infectious vectors	Vectors host^{-1}
W	Abundance of infectious vectors	Vectors host^{-1}
W_m	Abundance of immigrating infectious vectors	Vectors host^{-1}
S	Density of susceptible hosts	Hosts arena^{-1}
I	Density of infected hosts	Hosts arena^{-1}
H	Density of susceptible and infected hosts	Hosts arena^{-1}
n	Number of spatial classes of hosts	–
i	Index of spatial classes	–
r	Population growth rate of the vector	Day^{-1}
K	Carrying capacity of the vector	Vectors host^{-1}
d	Dispersal rate of the vector	Day^{-1}
β_{VH}	Transmission coefficient from vector to host	Hosts vector^{-1} day^{-1}
β_{HV}	Transmission coefficient from host to vector	Arenas host^{-1} day^{-1}
θ	Overdispersion of vectors among hosts	–

In the three scenarios, different spatiotemporal patterns arise because immigrating vectors (V_m and W_m) can arrive from different locations. In the *non-spatial* model ($n = 1$ spatial class),

$$V_{m,1} = V_1, \quad (5a)$$

$$W_{m,1} = W_1, \quad (5b)$$

so that immigration and emigration offset one another exactly, and vector dynamics follow pure logistic growth.

For *lagged dispersal* ($n = 2$ spatial classes),

$$V_{m,1} = V_{m,2} = V_1 \frac{H_1}{H_1 + H_2} + V_2 \frac{H_2}{H_1 + H_2}, \quad (6a)$$

$$W_{m,1} = W_{m,2} = W_1 \frac{H_1}{H_1 + H_2} + W_2 \frac{H_2}{H_1 + H_2}, \quad (6b)$$

where H_i is the sum of susceptible and infected hosts in each spatial class (H_i is a constant). Here, the total number of dispersing non-infectious vectors from both classes is $d(V_1H_1 + V_2H_2)$. This global pool of dispersing vectors is then distributed evenly among all hosts (i.e. vectors disperse globally), with a fraction $\frac{H_i}{H_1+H_2}$ immigrating into each spatial class i. This fraction weights net immigration by the relative abundance of hosts in each class so that each host receives the same number of immigrating vectors even if host densities differ between classes. Thus, the total number of non-infectious vectors dispersing into each class is $d(V_1H_1 + V_2H_2)\left(\frac{H_i}{H_1+H_2}\right)$, and the per-capita number of immigrating non-infectious vectors per individual host (after dividing by H_i) becomes $d\left(V_1\frac{H_1}{H_1+H_2} + V_2\frac{H_2}{H_1+H_2}\right)$ for both spatial classes (Equation 6a). Similar logic applies to the infectious vectors (Equation 6b). This *lagged dispersal* model converges with the *non-spatial* model as dispersal rates increase (Appendix; Figure S3).

Finally, for the *travelling wave* model ($n = 5$ spatial classes),

$$V_{m,i} = V_i \frac{H_i}{H_{i-1} + H_i + H_{i+1}} + V_{i-1} \frac{H_i}{H_{i-2} + H_{i-1} + H_i} + V_{i+1} \frac{H_i}{H_i + H_{i+1} + H_{i+2}}, \quad (7a)$$

$$W_{m,i} = W_i \frac{H_i}{H_{i-1} + H_i + H_{i+1}} + W_{i-1} \frac{H_i}{H_{i-2} + H_{i-1} + H_i} + W_{i+1} \frac{H_i}{H_i + H_{i+1} + H_{i+2}}, \quad (7b)$$

where vectors immigrate to new hosts from the current (i), preceding ($i - 1$) and succeeding classes ($i + 1$). The proportion of immigrating vectors that stay in their original class is the number of hosts in that class (H_i) relative to all new potential hosts ($H_i + H_{i+1} + H_{i-1}$). Thus, if the density of hosts increases between spatial classes ($H_{i+1} > H_i$, as in our

experiment), the pool of dispersing vectors is diluted among the larger subpopulation of new hosts. We assume reflecting boundary conditions by setting all densities of hosts and vectors outside of classes 1–5 equal to zero (e.g. $V_0 = V_6 = 0$). These assumptions cause different densities of vectors per host in each spatial class at extremely high dispersal rates (Appendix; Figure S4).

Importantly, environmental change—fertilisation in this case study—could impact disease dynamics by changing any of the parameters, including the vectors' population growth rate (r), carrying capacity (K), dispersal rate (d) or transmission from vector to host (β_{VH}; Figure 2).

2.4 | Model fitting

We fit all three models to the experiment using maximum likelihood (see Appendix for details). We simulated the models using the deSolve package in R version 3.5.2 (R Core Team, 2017; Soetaert et al., 2010), with starting conditions matching the experimental design. We fit these simulations to our data with the bbmle package (Bolker, 2008). We assumed that host infections (S or I) were distributed as Bernoulli variables. The aphid data were overdispersed relative to a Poisson distribution (the variance exceeded the mean), so we assumed that the total abundance of vectors per host ($V + W$) followed a negative binomial distribution and fit the degree of vector overdispersion (θ). In the global dispersal model, all observed data linked to the dynamics in the receiver class ($i = 2$); for the travelling wave model, data linked to spatial classes 2–5 (see Appendix for details). We were unable to fit both transmission coefficients, so we set transmission from host to vectors to a reasonable constant ($\beta_{HV} = 0.68$ arenas host^{-1} day^{-1} Jimenez-Martinez & Bosque-Perez, 2004). We estimated all of the other parameters (r, K, d, θ and β_{VH}) by searching likelihood surfaces with an optimiser with box constraints (L-BFGS-B). In the *lagged dispersal* model, dynamics on donor and receiver classes became indistinguishable when dispersal rates exceeded about 0.5 day^{-1} because excessive movement homogenised the spatial classes (Appendix; Figure S3). Since optimisers could not distinguish among dispersal rates in these scenarios, we set an upper limit of 0.5 on the estimation of d. We confirmed performance of our model fitting machinery by fitting models to simulated data (details in the Appendix; Figure S5).

We determined how environmental change shaped vector demography, dispersal and disease with a three-step model simplification (Table 2) and competition procedure (Table 3). This simplified procedure reduced the number of candidate models from 1,152 to 18. First, backwards simplification of the *non-spatial* model determined which non-spatial traits of vectors (r, K, θ and β_{VH}) differed with resource supply (R) or disease (D). If removing an effect did not substantially worsen model fit (ΔAIC < -5, compared to the full model with all treatment effects [model 1A]), then it was removed from the simplified model (model 1F). Second, we incorporated vector dispersal by competing this simplified *non-spatial* model against the *lagged dispersal* and *travelling wave* models, with all possible effects of resources and disease on dispersal rates (Table 3). Finally, we also considered a 'full' spatial model (model 3A) that reintroduced the previously omitted non-spatial terms. We determined the best model with AIC (Burnham & Anderson, 2002). When dispersal rate hit its upper limit (Figure S3), we calculated AIC with and without a penalty for d. We bootstrapped 95% confidence intervals around parameters of the best model (10,000 iterations; resampling hosts with replacement at each time, across arenas, within treatments), and used the bootstrapped distributions to assign post-hoc p values to treatment effects. For example, the p value for the effect of resources on carrying capacity (K) was the proportion of bootstrapped K's from the low resource treatment that exceeded the estimate of K with high resources. Since the bootstrapped distributions were skewed, we report the more conservative p value for each test.

TABLE 2 Simplification of the non-spatial model. The full model (model 1A; bold) includes all possible effects of resources (R) and disease (D) on traits of vectors (r, K, θ and β_{VH}). Each effect is removed individually (models 1B–1E; 1G–1I), with ΔAIC's calculated as differences from the full model. Generally, ΔAIC > 10 indicates poor model performance. The simplified non-spatial model (1F; bold) retains all important effects (individual ΔAIC's < -5), which are also included in the spatial models (Table 3)

Spatiotemporal scenario	Mod. ID	Model reduction	# Param.	AIC	ΔAIC	Removed from simplified model?
Non-spatial	**1A**	**Full model (all terms included)**	**14**	**5,108**	**0**	**—**
Non-spatial	1B	Without R → β_{VH}	13	4,836	1.7	Yes
Non-spatial	1C	Without R → θ	12	4,838	0.1	Yes
Non-spatial	1D	Without D → K	12	4,841	−3.3	Yes
Non-spatial	1E	Without D → θ	12	4,842	−4.5	Yes
Non-spatial	**1F**	**Simplified model**	**8**	**4,845**	**−7.2**	**—**
Non-spatial	1G	Without R → K	12	4,865	−27.2	No
Non-spatial	1H	Without R → r	12	4,880	−41.8	No
Non-spatial	1I	Without D → r	12	5,009	−171.2	No

TABLE 3 Model competition among spatiotemporal scenarios. Models include the simplified *non-spatial* model (model 1F; Table 2) and all possible effects of resources (R) and disease (D) on vector dispersal (*d*) in *lagged dispersal* and *travelling wave* models. A 'full' spatial model (model 3A) reintroduces the previously omitted non-spatial terms (Table 2). Models are sorted by AIC, with ΔAIC = 0 for the winning model (model 2A; bold)

Spatiotemporal scenario	Mod. ID	Model addition	# Param.	AIC	ΔAIC	Akaike weight, w[a]
Lagged dispersal	**2A**	**With R → *d* & D → *d***	**12**	**4,814**	**0**	**0.76 (0.76)**[b]
Lagged dispersal	3A	With R → *d*, β_{VH} & θ; D → *d*, *K* & θ	18	4,816	2.3	0.24 (0.24)
Lagged dispersal	2B	With R → *d*	10	4,825	11.8	2.1×10^{-3}
Lagged dispersal	2C	With D → *d*	10	4,833	19.0	5.8×10^{-5}
Lagged dispersal	2D	With single *d*	9	4,839	25.5	2.2×10^{-6}
Non-spatial	1F	Simplified *non-spatial* (Table 2)	8	4,845	31.4	1.1×10^{-7}
Travelling wave	2E	With D → *d*	10	5,164	350.3	6.5×10^{-77}
Travelling wave	2F	With R → *d* & D → *d*	12	5,167	353.6	1.3×10^{-77}
Travelling wave	2G	With single *d*	9	5,317	503.1	4.3×10^{-110}
Travelling wave	2H	With R → *d*	10	5,319	504.9	1.7×10^{-110}

[a]Akaike weights indicate the probability of a model being best among those considered.

[b]Parentheses indicate a less conservative *w*, with AIC's not penalised for the dispersal parameter *d* when it hit its upper limit (# parameters = *n*−1 for models 2A, 3A and 2B).

3 | RESULTS

In the experiment, vector populations grew rapidly and plateaued as aphids reproduced and dispersed among hosts (Figure 3a,b,d,e). All host plants in treatments with the virus became infected within 8 weeks (Figure 3c,f). We confirmed that all hosts in treatments without the virus remained uninfected. We detected very few winged aphids (32 of 33,000 sampled aphids, <0.1%, mostly at the end of the experiment), indicating that transmission occurred predominantly as aphid vectors crawled between hosts.

Vector demography in the *non-spatial* model differed with both resource supply and disease (Table 1). Carrying capacity of the vector (*K*) responded to resource supply (model 1G; ΔAIC = −27.2), and growth rate (*r*) responded to both resource supply (model 1H; ΔAIC = −41.8) and disease (model 1I; ΔAIC = −171.2). All other terms were removed from the simplified *non-spatial* model (model 1F; ΔAIC = −7.2) and all subsequent spatial models (except model 3A).

The *lagged dispersal* model best explained spatial dynamics of the experiment, with dispersal rates (*d*) differing with both resource supply and disease (models 2A and 3A). Thus, vectors first reproduced on 'donor' hosts before dispersing to other 'receiver' hosts in the arenas, and infection prevalence in the receiver hosts lagged behind the donors (Figure 3c). The second-ranking model reintroduced all of the 'unimportant' non-spatial terms, but did not improve model fit (model 3A; ΔAIC = 2.3). We therefore preferred the simpler of these two models (model 2A). These two models vastly outperformed all others (Table 3). Their Akaike weights (*w*: probability of being best among the models tested) were 0.76 and 0.24, respectively, with quantitatively similar AIC scores with and without a penalty for the parameter *d* when it reached its upper limit (Table 3). The *lagged dispersal* model fit substantially worse when dispersal rates varied only with resources (model 2B; $w = 2.1 \times 10^{-3}$) or disease (model 2C; $w = 5.8 \times 10^{-5}$). Thus, resource supply and disease together altered vector dispersal. The simplified *non-spatial* model fit even more poorly (model 1F; $w = 1.1 \times 10^{-7}$), despite requiring fewer parameters, and underestimated the population growth rate of vectors (*r*) by as much as 34% (Appendix; Figure S6; Table S2). Fit of the *travelling wave* model was the worst (models 2E–H; all $w < 10^{-76}$), indicating that vectors and infections did not spread across the arenas in travelling waves (Figure S6).

The best-fitting *lagged dispersal* model flexibly distinguished among differences in population growth rates (*r*), carrying capacities (*K*) and dispersal rates of vectors (*d*; Figure 2; Figure S7). Post-hoc comparisons confirmed how resource supply and disease altered these demographic and behavioural traits of vectors. Population growth rates of vectors decreased with resource supply (Figure 4a), both with disease ($p = 0.034$) and without ($p = 0.020$). Population growth rates also decreased with disease, significantly with high resource supply ($p = 0.021$) and marginally with low resource supply ($p = 0.060$). The carrying capacity of vectors per host increased dramatically, nearly doubling with higher resource supply (Figure 4b; $p < 0.0001$). Dispersal rate of vectors was clearly slowest in treatments that combined disease and low resource supply (Figure 4c). In the other treatments, dispersal rates overlapped with the upper limit of *d*, making the *lagged dispersal* and *non-spatial* models indistinguishable. In other words, with high resource supply and/or absence of disease, dispersal rates were rapid enough justify using the simpler *non-spatial* model. However, with low resource supply and disease, dispersal rates were substantially slower ($p < 0.0001$).

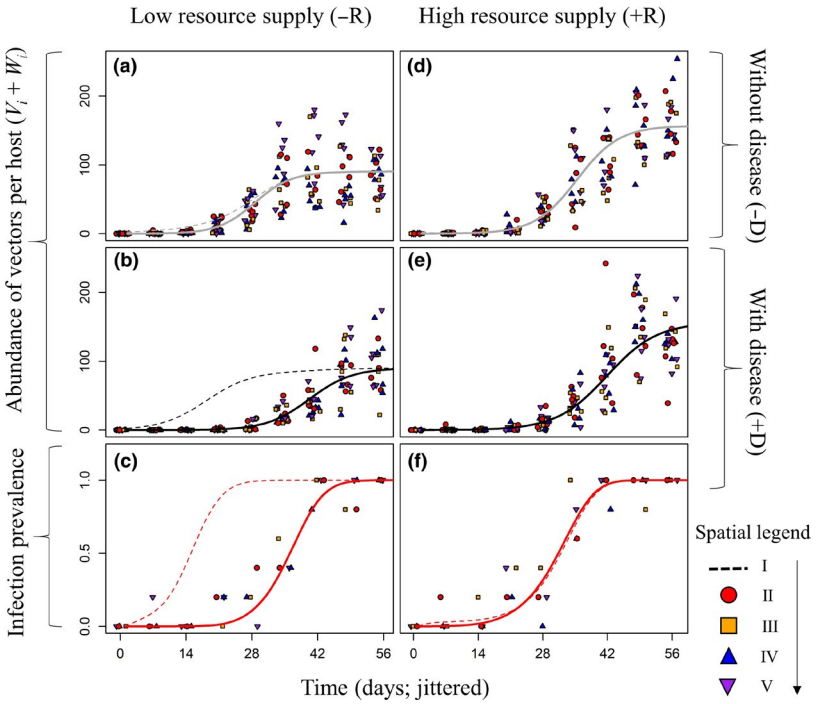

FIGURE 3 The spread of vectors and infections in experimental arenas. The best model (*lagged dispersal*; model 2A; Table 3) is fit to each treatment. **Low resource supply** (left): Vectors grow logistically in the absence (a) or presence of disease (b). Without disease, dynamics are nearly indistinguishable on donor (dashed line) and receiver hosts (solid line). With disease, vectors disperse slower, and abundances on receiver hosts lag behind. (c) All hosts become infected, with a corresponding lag between infection prevalence in the donor (dashed) and receiver hosts (solid). **High resource supply** (right): Vectors reach higher carrying capacities with elevated resource supply, both without (d) and with disease (e). Fast dispersal rates homogenise vector dynamics on donor and receiver hosts (overlapping dashed and solid lines). (f) Disease risk is also spatially homogenised, with all hosts rapidly becoming infected (no lag in infection prevalence between classes). Key to spatial structure: Hosts radiate outward from the centre (I; no data) to rings II (red circles), III (orange squares), IV (blue upwards triangles) and V (purple downward triangles)

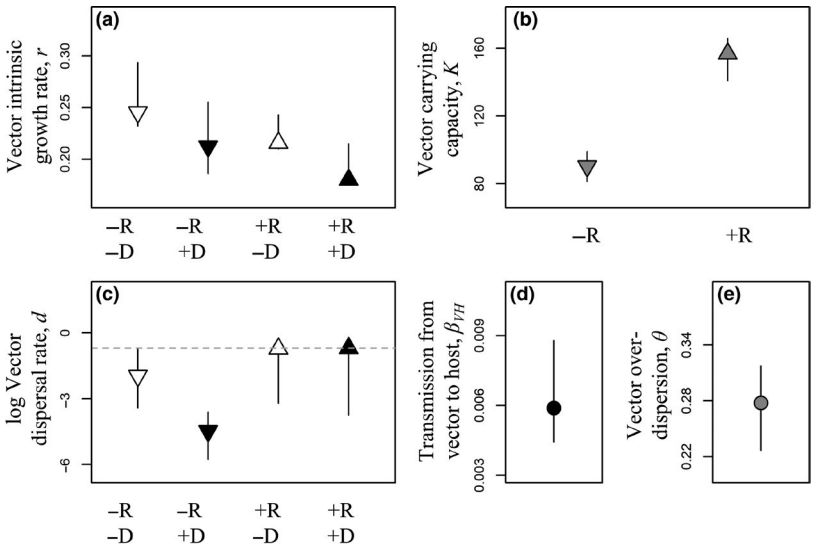

FIGURE 4 Effects of resources (±R) and disease (±D) on vector demography and dispersal. Points show traits of vectors (fitted parameters from the best *lagged dispersal* model; model 2A) with bootstrapped 95% confidence intervals. (a) **Population growth rate** (r) decreases with higher resource supply and presence of the pathogen (note the right-skew on the bootstrapped distributions). (b) **Carrying capacity** of the vector (K) increases with resource supply. (c) **Dispersal rate** (d) is slowest with the combination of low resources and disease. In other treatments, dispersal rates are high enough (horizontal dashed line) that the *lagged dispersal* and *non-spatial* models become indistinguishable. Neither (d) **transmission** from vector to host (β_{HV}) nor (e) **vector overdispersion** (θ) differ among treatments (Table 2). Key: shapes = resource level (upward triangles = high; downward triangles = low; circles = both); shading = disease (white = without; black = with; grey = both)

4 | DISCUSSION

The transmission of arthropod-vectored diseases across space depends on vector demography and dispersal. Although foundational models of vectored diseases often assume frequency-dependent transmission (Antonovics et al., 1995; Chan & Jeger, 1994), more recent models that explicitly track vector dynamics have led to new insights and predictions (Chao et al., 2013; Crowder et al., 2019; Shoemaker et al., 2019). However, these models are rarely paired with experiments that test how environmental change shapes disease via vector ecology. Here, we developed models for three scenarios: a *non-spatial* transmission model, *lagged dispersal* of vectors across space and a *travelling wave*. We asked how environmental eutrophication (fertilisation of plant hosts) altered vector demography and dispersal and the spread of disease in experimental arenas. The *lagged dispersal* model provided the strongest fit to the data, indicating that vectors first reproduced on an initial 'donor' class of hosts and then dispersed globally to all others. Vector carrying capacity (*K*) nearly doubled with resource supply, population growth rates (*r*) decreased with both resource supply and disease, and dispersal rates (*d*) were slowest with the combination of low resource supply and disease. This model and experiment emphasise the importance of vector demography and dispersal for the transmission of disease over space and time, especially under conditions of environmental change.

The simplest, *non-spatial* model adequately described dynamics in three of four treatments, but the *lagged dispersal* model became essential with low resource supply and disease. Ignoring space in disease models is tempting because it simplifies predictions and enables analytical tractability (Keeling et al., 2007; Shaw et al., 2019). Here, space became important with presence of the virus and low resource supply to hosts. Together, these treatments constrained vector populations by allowing relatively slow population growth rates (*r*), low carrying capacities (*K*) and slow dispersal rates (*d*). Under these conditions, dispersal of vectors across space—after a period of initial reproduction—played a key role in structuring the spatial distribution of vectors and infections. Notably, infection prevalence in receiver hosts lagged 2 weeks behind infection prevalence in the donors. The simpler *non-spatial* model badly underestimated vector population growth rate (by 34%) and failed to capture this spatial lag. In the arenas with elevated resource supply, faster aphid dispersal rates homogenised disease risk across space. This increase in dispersal rate may reflect changes in plant growth and physiology: Fertilised plants were larger with more overlapping leaves, likely promoting aphid movement and disease spread. Broadly, these results suggest that space and movement could become more important features of disease models when environmental conditions exert stronger constraints on vector demography and dispersal.

Higher environmental resource supply decreased aphid population growth rates (*r*) but nearly doubled the carrying capacity of aphids per plant (*K*). Each of these effects could shape disease more strongly at different spatial scales. Aphid fecundity often increases with nitrogen (Borer et al., 2009), but nitrogen can also slow aphid growth rates (Bogaert et al., 2017) especially in combination with phosphorus (Zehnder & Hunter, 2009). These results suggest that elevated resources (especially phosphorus) may allow plants to mount stronger defences against aphids. Presence of the virus also reduced aphid growth rates in the arenas, which was atypical (Bosque-Perez & Eigenbrode, 2011) but not unusual (Jimenez-Martinez et al., 2004). Despite slower initial population growth, aphids reached higher carrying capacities (*K*) on fertilised plants. Populations of other vectors may be similarly limited by the resources of their hosts. Ticks are especially abundant after masting years with high acorn production (Ostfeld et al., 1996); kissing bugs are more common in palms growing in richer soils (Abad-Franch et al., 2010) and more mosquitos emerge from eutrophic wetlands (Pope et al., 2005; Schrama et al., 2018). In the arenas, most hosts became infected before aphids reached their carrying capacity. Thus, at this scale (i.e. early stages of an epidemic), effects of resources on *r* might shape disease more strongly than effects on *K*. However, effects on carrying capacity could become more important at broader scales because more aphids dispersing away from infected plants could fuel more expansive epidemics (Comeau & Dubuc, 1977; Hamback et al., 2007). Thus, environmental change can have contrasting effects on short-term (*r*) and long-term vector demography (*K*), and implication of these effects for disease may vary by scale.

The three models developed here could also become more or less appropriate at different scales. The *lagged dispersal* model provided the best overall fit to the experimental arenas, which were relatively small populations of 100 hosts. The *non-spatial* model also seemed adequate when aphids dispersed rapidly, and could predict disease dynamics at smaller spatial scales, longer timescales, or if vectors disperse greater distances. The *travelling wave* model fit universally poorly, likely reflecting the small size of the arenas relative to aphids' ability to disperse among hosts (Bailey et al., 1995). However, at much broader spatial scales of agricultural fields, travelling waves of infection emanate outward from primary BYDV infections (Comeau & Dubuc, 1977; Irwin & Thresh, 1990). Similar waves of insects and pathogens have spread across forests (Bjørnstad et al., 2002; Evans, 2016; Menkis et al., 2016). Travelling waves have also been detected for dengue, a mosquito-borne virus in humans (Cummings et al., 2004) and tick-borne diseases have been linked to transmission at multiple scales due to movement of both vectors and hosts (Foley et al., 2016; Walter et al., 2016). Thus, qualitatively different spatiotemporal disease patterns can emerge for vectored diseases, depending on (a) the space occupied by the host population, (b) the relative distance over which vectors (and/or hosts) disperse and (c) the lag time required for vector feeding and/or reproduction.

The small, tractable scale of the arenas allowed us to fit key parameters for dynamical disease models (*r*, *K*, *d* and β_{HV}) and ask how these vector traits varied with experimental eutrophication. One limitation of this approach is that extension of these models to broader spatial scales may require more refined assumptions about vector dispersal. Per-capita dispersal can remain constant (Lombaert et al., 2006) or increase with aphid density (Tokunaga & Suzuki, 2008). Our simplifying assumption of constant dispersal rates seemed reasonable since most transmission in the arenas occurred before aphids reached high densities. At larger scales (e.g. in natural systems), this assumption could be more consequential. For example, models show that increasingly density-dependent dispersal can slow disease spread (Shaw et al., 2017), and

that elevated carrying capacity can accelerate spread under these conditions. In the experiment, we were also able to ignore winged aphids (alates) and dispersal distances, because alates were extremely rare and crawling (apterous) aphids dispersed globally within the arena. Yet, alates are critical for long-distance viral spread (Donnelly et al., 2019; Irwin & Thresh, 1988), and apterous aphids can crawl surprisingly far (Bailey et al., 1995). Thus, extensions of this framework to broader spatial scales would require additional experiments to ask how resource supply rates affect the density dependence of dispersal, the production of alates and the maximum dispersal distances of both alates and apterous aphids.

Insects are critical for the spatiotemporal spread of vectored diseases, but key components of vector ecology, such as their demography, dispersal and responses to environmental change, remain understudied in theory and experiments. Here, we emphasised the importance of vector reproduction and dispersal relative to the spatial scale of host populations, especially in light of relevant environmental change. The fields of population biology and behavioural ecology each have deep theoretical and empirical lineages, and infusing these perspectives into disease ecology is sure to lead to new questions and promising frontiers.

ACKNOWLEDGEMENTS

N. Venkateswaran and A. Cheng helped sample the experiment. A. Sieben led infection diagnosis work. Discussions with L. Shoemaker helped frame the results. Support was funded by NSF IOS 1556674 to A.K.S., E.T.B., and E.W.S. and NSF DEB 1556649 to E.W.S. and E.T.B.

AUTHORS' CONTRIBUTIONS

A.T.S. designed the models with feedback from A.K.S., E.T.B. and E.W.S.; A.T.S., E.T.B. and E.W.S. designed the experiment; A.T.S., J.A.H., A.P.-K. and A.L.A. conducted the experiment; A.T.S. wrote the first draft of the paper, and all authors contributed to revisions.

DATA AVAILABILITY STATEMENT

All data have been deposited in the Dryad Digital Repository https://doi.org/10.5061/dryad.5x69p8d1g (Strauss et al., 2020).

ORCID

Alexander T. Strauss https://orcid.org/0000-0003-0633-8443
Jeremiah A. Henning https://orcid.org/0000-0002-2214-4895
Anita Porath-Krause https://orcid.org/0000-0002-9119-2372
Ashley L. Asmus https://orcid.org/0000-0001-5505-1372
Allison K. Shaw https://orcid.org/0000-0001-7969-8365
Elizabeth T. Borer https://orcid.org/0000-0003-2259-5853
Eric W. Seabloom https://orcid.org/0000-0001-6780-9259

REFERENCES

Abad-Franch, F., Ferraz, G., Campos, C., Palomeque, F. S., Grijalva, M. J., Aguilar, H. M., & Miles, M. A. (2010). Modeling disease vector occurrence when detection is imperfect: Infestation of Amazonian palm trees by triatomine bugs at three spatial scales. *PLoS Neglected Tropical Diseases*, *4*, e620. https://doi.org/10.1371/journal.pntd.0000620

Antonovics, J., Iwasa, Y., & Hassell, M. P. (1995). A generalized model of parasitoid, venereal, and vector-based transmission processes. *The American Naturalist*, *145*, 661–675. https://doi.org/10.1086/285761

Bailey, S. M., Irwin, M. E., Kampmeier, G. E., Eastman, C. E., & Hewings, A. D. (1995). Physical and biological perturbations – Their effect on the movement of apterous *Rhopalosiphum padi* (Homoptera, Aphididae) and localized spread of barley yellow dwarf virus. *Environmental Entomology*, *24*, 24–33.

Bjørnstad, O. N., Peltonen, M., Liebhold, A. M., & Baltensweiler, W. (2002). Waves of larch budmoth outbreaks in the European Alps. *Science*, *298*, 1020–1023. https://doi.org/10.1126/science.1075182

Bogaert, F., Chesnais, Q., Catterou, M., Rambaud, C., Doury, G., & Ameline, A. (2017). How the use of nitrogen fertiliser may switch plant suitability for aphids: The case of Miscanthus, a promising biomass crop, and the aphid pest Rhopalosiphum maidis. *Pest Management Science*, *73*, 1648–1654.

Bolker, B. M. (2008). *Ecological models and data in R*. Princeton, NJ: Princeton University Press.

Borer, E. T., Adams, V. T., Engler, G. A., Adams, A. L., Schumann, C. B., & Seabloom, E. W. (2009). Aphid fecundity and grassland invasion: Invader life history is the key. *Ecological Applications*, *19*, 1187–1196. https://doi.org/10.1890/08-1205.1

Bosque-Perez, N. A., & Eigenbrode, S. D. (2011). The influence of virus-induced changes in plants on aphid vectors: Insights from luteovirus pathosystems. *Virus Research*, *159*, 201–205. https://doi.org/10.1016/j.virusres.2011.04.020

Burnham, K. P., & Anderson, D. R. (2002). *Model selection and inference: A practical information-theoretic approach*. New York, NY: Springer-Verlag.

Chamchod, F., & Britton, N. F. (2011). Analysis of a vector-bias model on malaria transmission. *Bulletin of Mathematical Biology*, *73*, 639–657. https://doi.org/10.1007/s11538-010-9545-0

Chan, M. S., & Jeger, M. J. (1994). An analytical model of plant-virus disease dynamics with roguing and replanting. *Journal of Applied Ecology*, *31*, 413–427. https://doi.org/10.2307/2404439

Chao, D. L., Longini, I. M., & Halloran, M. E. (2013). The effects of vector movement and distribution in a mathematical model of dengue transmission. *PLoS ONE*, *8*, e76044. https://doi.org/10.1371/journal.pone.0076044

Comeau, A., & Dubuc, J. P. (1977). Observations on the 1976 barley yellow dwarf epidemic in Eastern Canada. *Canadian Plant Disease Survey*, *57*, 42–44.

Crowder, D. W., Li, J., Borer, E. T., Finke, D. L., Sharon, R., Pattemore, D. E., & Medlock, J. (2019). Species interactions affect the spread of vector-borne plant pathogens independent of transmission mode. *Ecology*, *100*, e02782. https://doi.org/10.1002/ecy.2782

Cummings, D. A. T., Irizarry, R. A., Huang, N. E., Endy, T. P., Nisalak, A., Ungchusak, K., & Burke, D. S. (2004). Travelling waves in the occurrence of dengue haemorrhagic fever in Thailand. *Nature*, *427*, 344–347. https://doi.org/10.1038/nature02225

Donnelly, R., Cunniffe, N. J., Carr, J. P., & Gilligan, C. A. (2019). Pathogenic modification of plants enhances long-distance dispersal of nonpersistently transmitted viruses to new hosts. *Ecology*, *100*, e02725. https://doi.org/10.1002/ecy.2725

Evans, A. M. (2016). The speed of invasion: Rates of spread for thirteen exotic forest insects and diseases. *Forests*, *7*, 1–11. https://doi.org/10.3390/f7050099

Foley, J., Rejmanek, D., Foley, C., & Matocq, M. (2016). Fine-scale genetic structure of woodrat populations (Genus: Neotoma) and the spatial distribution of their tick-borne pathogens. *Ticks and Tick-Borne Diseases*, *7*, 243–253. https://doi.org/10.1016/j.ttbdis.2015.10.017

Githeko, A. K., Lindsay, S. W., Confalonieri, U. E., & Patz, J. A. (2000). Climate change and vector-borne diseases: A regional analysis. *Bulletin of the World Health Organization*, *78*, 1136–1147.

Hamback, P. A., Vogt, M., Tscharntke, T., Thies, C., & Englund, G. (2007). Top-down and bottom-up effects on the spatiotemporal dynamics

of cereal aphids: Testing scaling theory for local density. *Oikos*, *116*, 1995–2006. https://doi.org/10.1111/j.2007.0030-1299.15800.x

Hastings, A., Cuddington, K., Davies, K. F., Dugaw, C. J., Elmendorf, S., Freestone, A., … Thomson, D. (2005). The spatial spread of invasions: New developments in theory and evidence. *Ecology Letters*, *8*, 91–101. https://doi.org/10.1111/j.1461-0248.2004.00687.x

Irwin, M. E., & Thresh, J. M. (1988). Long-range aerial dispersal of cereal aphids as virus vectors in North America. *Philosophical Transactions of the Royal Society of London. B: Biological Sciences*, *321*, 421–446.

Irwin, M. E., & Thresh, J. M. (1990). Epidemiology of barley yellow dwarf – A study in ecological complexity. *Annual Review of Phytopathology*, *28*, 393–424. https://doi.org/10.1146/annurev.py.28.090190.002141

Jeger, M. J., Madden, L. V., & van den Bosch, F. (2018). Plant virus epidemiology: Applications and prospects for mathematical modeling and analysis to improve understanding and disease control. *Plant Disease*, *102*, 837–854. https://doi.org/10.1094/PDIS-04-17-0612-FE

Jimenez-Martinez, E. S., & Bosque-Perez, N. A. (2004). Variation in barley yellow dwarf virus transmission efficiency by *Rhopalosiphum padi* (Homoptera: Aphididae) after acquisition from transgenic and non-transformed wheat genotypes. *Journal of Economic Entomology*, *97*, 1790–1796. https://doi.org/10.1093/jee/97.6.1790

Jimenez-Martinez, E. S., Bosque-Perez, N. A., Berger, P. H., & Zemetra, R. S. (2004). Life history of the bird cherry-oat aphid, *Rhopalosiphum padi* (Homoptera: Aphididae), on Transgenic and untransformed wheat challenged with Barley yellow dwarf virus. *Journal of Economic Entomology*, *97*, 203–212.

Keeling, M., Rohani, P., & Pourbohloul, B. (2007). *Modeling infectious diseases in humans and animals*. Princeton, NJ: Princeton University Press.

Kingsolver, J. G. (1987). Mosquito host choice and the epidemiology of malaria. *The American Naturalist*, *130*, 811–827. https://doi.org/10.1086/284749

Lacroix, C., Seabloom, E. W., & Borer, E. T. (2014). Environmental nutrient supply alters prevalence and weakens competitive interactions among coinfecting viruses. *New Phytologist*, *204*, 424–433. https://doi.org/10.1111/nph.12909

Lombaert, E., Boll, R., & Lapchin, L. (2006). Dispersal strategies of phytophagous insects at a local scale: Adaptive potential of aphids in an agricultural environment. *BMC Evolutionary Biology*, *6*, 75.

Madden, L. V., Jeger, M. J., & van den Bosch, F. (2000). A theoretical assessment of the effects of vector-virus transmission mechanism on plant virus disease epidemics. *Phytopathology*, *90*, 576–594. https://doi.org/10.1094/PHYTO.2000.90.6.576

Marini, F., Caputo, B., Pombi, M., Tarsitani, G., & Della Torre, A. (2010). Study of Aedes albopictus dispersal in Rome, Italy, using sticky traps in mark-release-recapture experiments. *Medical and Veterinary Entomology*, *24*, 361–368.

Menkis, A., Ostbrant, I. L., Wagstrom, K., & Vasaitis, R. (2016). Dutch elm disease on the island of Gotland: Monitoring disease vector and combat measures. *Scandinavian Journal of Forest Research*, *31*, 237–241. https://doi.org/10.1080/02827581.2015.1076888

Ostfeld, R. S., Jones, C. G., & Wolf, J. O. (1996). Of mice and mast. *BioScience*, *46*, 323–330. https://doi.org/10.2307/1312946

Pope, K., Masuoka, P., Rejmankova, E., Grieco, J., Johnson, S., & Roberts, D. (2005). Mosquito habitats, land use, and malaria risk in Belize from satellite imagery. *Ecological Applications*, *15*, 1223–1232. https://doi.org/10.1890/04-0934

R Core Team. (2017). *R: A language and environment for statistical computing*. Vienna, Austria: R Foundation for Statistical Computing.

Russell, R. C., Webb, C. E., Williams, C. R., & Ritchie, S. A. (2005). Mark-release-recapture study to measure dispersal of the mosquito Aedes aegypti in Cairns, Queensland, Australia. *Medical and Veterinary Entomology*, *19*, 451–457. https://doi.org/10.1111/j.1365-2915.2005.00589.x

Schrama, M., Gorsich, E. E., Hunting, E. R., Barmentlo, S. H., Beechler, B., & van Bodegom, P. M. (2018). Eutrophication and predator presence overrule the effects of temperature on mosquito survival and development. *PLoS Neglected Tropical Diseases*, *12*, 13. https://doi.org/10.1371/journal.pntd.0006354

Seabloom, E. W., Borer, E. T., Lacroix, C., Mitchell, C. E., & Power, A. G. (2013). Richness and composition of niche-assembled viral pathogen communities. *PLoS ONE*, *8*, e55675. https://doi.org/10.1371/journal.pone.0055675

Shaw, A. K., Igoe, M., Power, A. G., Bosque-Pérez, N. A., & Peace, A. (2019). Modeling approach influences dynamics of a vector-borne pathogen system. *Bulletin of Mathematical Biology*, *81*, 2011–2028. https://doi.org/10.1007/s11538-019-00595-z

Shaw, A. K., Peace, A., Power, A. G., & Bosque-Pérez, N. A. (2017). Vector population growth and condition-dependent movement drive the spread of plant pathogens. *Ecology*, *98*, 2145–2157. https://doi.org/10.1002/ecy.1907

Shoemaker, L. G., Hayhurst, E., Weiss-Lehman, C. P., Strauss, A. T., Porath-Krause, A., Borer, E. T., … Shaw, A. K. (2019). Pathogens manipulate the preference of vectors, slowing disease spread in a multi-host system. *Ecology Letters*, *22*, 1115–1125. https://doi.org/10.1111/ele.13268

Skellam, J. G. (1951). Random dispersal in theoretical populations. *Bulletin of Mathematical Biology*, *53*, 135–165. https://doi.org/10.1016/S0092-8240(05)80044-8

Soetaert, K., Petzoldt, T., & Setzer, R. W. (2010). Solving differential equations in R: Package deSolve. *Journal of Statistical Software*, *33*, 1–25.

Sota, T., & Mogi, M. (1989). Effectiveness of zooprophylaxis in malaria control – A theoretical inquiry, with a model for mosquoti populations with two bloodmeal hosts. *Medical and Veterinary Entomology*, *3*, 337–345.

Strauss, A. T., Henning, J. A., Porath-Krause, A., Asmus, A. L., Shaw, A. K., Borer, E. T., & Seabloom, E. W. (2020). Data from: Vector demography, dispersal and the spread of disease: Experimental epidemics under elevated resource supply. *Dryad Digital Repository*, https://doi.org/10.5061/dryad.5x69p8d1g

Tokunaga, E., & Suzuki, N. (2008). Colony growth and dispersal in the ant-tended aphid, *Aphis craccivora* Koch, and the non-ant-tended aphid, *Acyrthosiphon pisum* Harris, under the absence of predators and ants. *Population Ecology*, *50*, 45–52. https://doi.org/10.1007/s10144-007-0065-1

Walter, K. S., Pepin, K. M., Webb, C. T., Gaff, H. D., Krause, P. J., Pitzer, V. E., & Diuk-Wasser, M. A. (2016). Invasion of two tick-borne diseases across New England: Harnessing human surveillance data to capture underlying ecological invasion processes. *Proceedings of the Royal Society B: Biological Sciences*, *283*, 20160834. https://doi.org/10.1098/rspb.2016.0834

Zehnder, C. B., & Hunter, M. D. (2009). More is not necessarily better: The impact of limiting and excessive nutrients on herbivore population growth rates. *Ecological Entomology*, *34*, 535–543. https://doi.org/10.1111/j.1365-2311.2009.01101.x

SUPPORTING INFORMATION

Additional supporting information may be found online in the Supporting Information section.

How to cite this article: Strauss AT, Henning JA, Porath-Krause A, et al. Vector demography, dispersal and the spread of disease: Experimental epidemics under elevated resource supply. *Funct Ecol*. 2020;34:2560–2570. https://doi.org/10.1111/1365-2435.13672